A Study of Multifunctional Slope Adaptive Behaviors in Ankle Prostheses

By

Pierce Finley

Thesis

Submitted to the Faculty of the

Graduate School of Vanderbilt University

in partial fulfillment of the requirements

for the degree of

MASTER OF SCIENCE

in

Mechanical Engineering

August 9, 2019

Nashville, Tennessee

Approved:

Michael Goldfarb, Ph.D.

Karl Zelik, Ph.D.

David Braun, Ph.D.

To the glory of God and to my parents,

to whom I owe everything

Table of Contents

List of Tables

Page

List of Figures

Page

Introduction

There has been a large increase in the variety and functionality of transtibial prostheses, both in the development of new designs for passive prostheses and as a result of the modern expansion of efficient electromechanical systems. These prostheses, more complex and providing more differences in behavior than simple springs, will be referred to generally as "multifunctional" prostheses throughout this paper. Fixed carbon fiber leaf spring foot-ankle prostheses, however, remain the standard in transtibial prostheses. They excel in light weight, relatively lower cost, and ease of use for many simple everyday tasks. In their simplicity, they are fixed to a single angle and stiffness, which can limit their ability to adapt to uneven or sloped terrain. As more multifunctional prostheses are developed in research and sold commercially with slope-adaptive behaviors, it is valuable to empirically assess the tradeoffs of providing these behaviors compared to a simple spring. Some examples of these multifunctional prostheses and their additional capabilities are shown in Figure 1.

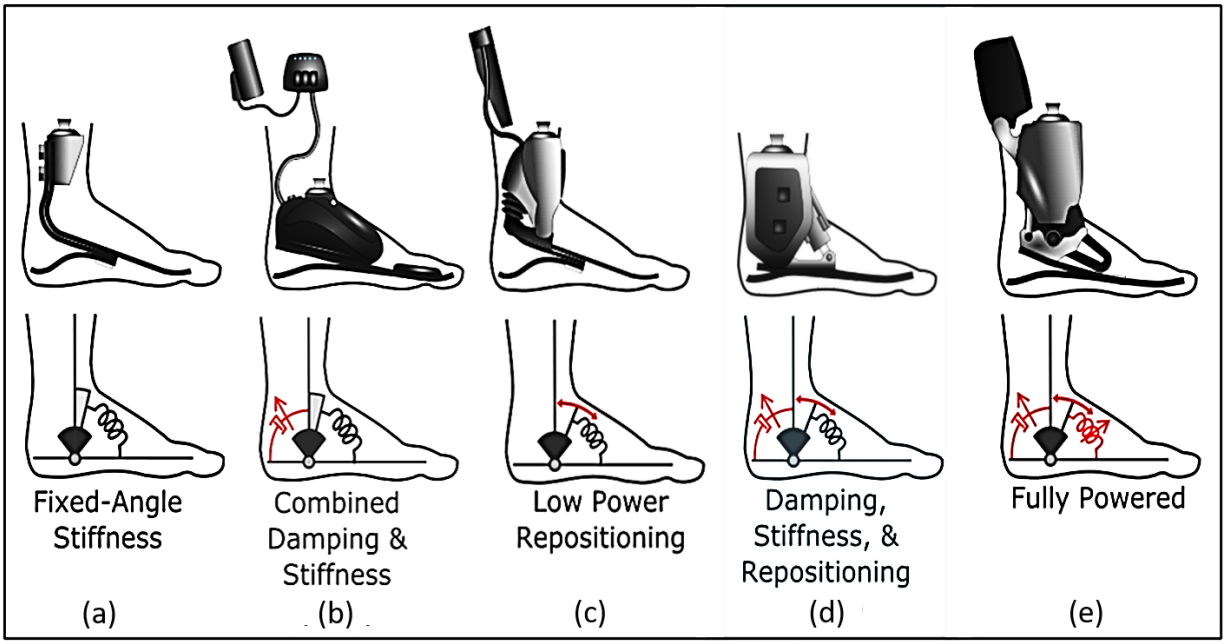

Figure 1. Summary of multifunctional prostheses compared to basic spring. Red features indicate those controlled by a microcontroller.

The focus of this thesis is to evaluate three ankle behaviors; namely, to evaluate the level and sloped walking characteristics of two multifunctional ankle behaviors relative to the standard fixed angle stiffness ankle. The first multifunctional ankle behavior is the addition of a region of hydraulic damping in the ankle's mid-stance range of

motion. Foot-ankle systems such as the Fillauer Raize and Endolite Echelon have incorporated this behavior in part to enhance ground conformation and alleviate socket discomfort during sloped standing and walking.

The second multifunctional behavior includes a region of conformal damping similar to the first multifunctional behavior, along with equilibrium angle adjustment as described in [1]. This control scheme ads hydraulic damping in early and mid-stance, but also can adapt the push-off spring equilibrium angle to the ground slope with each step. These two multifunctional behaviors are represented by (b) and (d) in Figure 1.

In order to determine the specific biomechanical benefits of multifunctional prostheses, particularly those with conformal damping behavior, several studies have been conducted [2-12]. The majority of these studies focus on level ground walking [2-6], with several also dedicated to sloped walking [7-11]. In particular, it has been found that conformal damping can reduce joint loading in sloped walking [7], reduce the braking done in early stance to improve rollover [2], and increase the negative work done by the prosthetic ankle joint in ramp descent [10], all of which can contribute to healthy gait. It has also been shown that they can provide an improved trajectory for the center of pressure under the prosthetic foot during stance [3]. However, some studies have reported insignificant differences, such as [9] which reported no statistically significant change in the moment acting at the socket connection.

Although some previous studies have considered the improvement in comfort afforded by conformal damping, as well as joint loading and other kinetic analysis, they often neglect the effects of such damping on energy return. This study characterizes the effects of conformal damping on comfort and energy return, in addition to step symmetry, relative to fixed angle stiffness devices. Further, this study also compares these to a third case, which is a unique controller that incorporates conformal damping, in addition to a ground-slope adaptive stiffness equilibrium point. It is predicted that adding a damping phase that shifts the spring equilibrium angle to a more dorsiflexed position will reduce the energy return as well as the symmetry of step length, while being able to adjust the equilibrium angle to the slope will help offset some of these differences and provide an energy return and symmetry similar to a constant spring foot. The damping should also reduce the overall torque loading at the socket, possibly accounting for more comfort and stability.

Multifunctional Behaviors and Experimental Emulation

Powered Ankle Prosthesis Emulator

Rather than test each behavior on a different device, the three ankle behaviors tested here (fixed stiffness, conformal damping with stiffness, and conformal damping with slope adaptive equilibrium) were implemented in a robotic prosthesis emulator, which is discussed more in depth in [13]. The ankle used for this study is a more recent iteration than that discussed in [13], with the embedded system updated to fit on-board and an improved battery pack, but the mechanical properties are equivalent. Shown in Figure 2, this device is a robust system driven by a Maxon EC60 flat brushless motor connected to a 116:1 transmission. It is capable of producing a torque of approximately 100 Nm with this motor and transmission. It is also equipped with a foot possessing a parallel carbon fiber leaf spring that engages at approximately 0° to add up to 50 Nm of plantarflexion torque when the ankle itself is dorsiflexed.

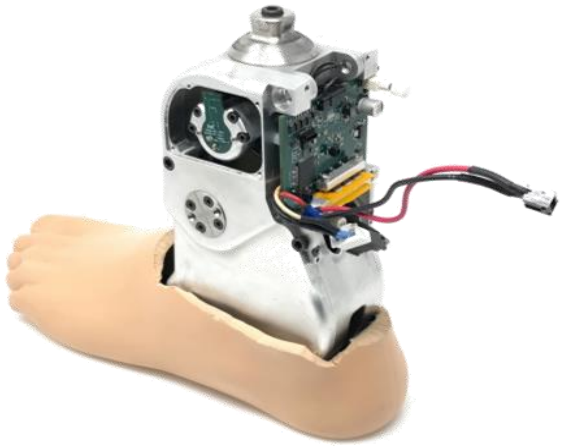

Figure 2. Vanderbilt University powered transtibial prosthesis

For all ankle controllers implemented in this study, the overall control method is a torque based approach. The torque is determined with a simple spring-damper calculation shown in (1).

$$\tau = k\left(\theta - \theta_{eq}\right) + b\dot{\theta} \tag{1}$$

where τ is ankle torque, θ and $\dot{\theta}$ are ankle angle and angular velocity, k and b are the spring constant and damping coefficient, and θ_{eq} is the equilibrium angle. At any given moment in the gait cycle, the torque behavior is controlled by setting the value of k, b, and θ_{eq}. Since the actual implementation includes an additional carbon fiber leaf spring in dorsiflexion, there is another term included in the final torque calculation to compensate for this additional spring

torque. This term is never changed by the higher level control.

By using the same device for all behaviors, we control for factors such as weight and foot shape. This allows us to isolate the controller behaviors rather than other aspects of the prosthesis design. The controllers employed for each implementation are described below.

Multifunctional Controllers

The three controllers selected represent increasing design complexity and increasing functionality. The simplest control scheme is a constant spring behavior. A stiffness is selected by the participant for level ground walking (primarily determined by desired push off force) and kept constant for all testing conditions. A very slight damping is introduced to prevent large oscillations during swing phase, but the dominant behavior is that of an angular spring. The equilibrium angle of this spring is selected to be near 0°, and it is also held constant for all conditions. This controller will be referred to as "Controller A".

The second control scheme introduces an exclusively damped stage into the gait cycle. During mid-stance – from 6° plantarflexed to 3° dorsiflexed – the spring constant is reduced to zero and the damping coefficient is increased. Outside this range, the damping is again reduced and the spring behavior is re-engaged, using the boundaries of the mid-stance region as the equilibrium angles. This is to imitate several hydraulic-based prostheses that provide damping in mid-stance with hard stops to maintain a spring behavior outside this range. The plantar- and dorsiflexed spring regions use the same spring constant as the Controller A stiffness setting. The transitions of these parameters during walking was controlled via a finite state machine (FSM), as shown in Figure 3. A swing phase adjustment was included to prevent frequent toe scuffing. This controller will be referred to as "Controller B".

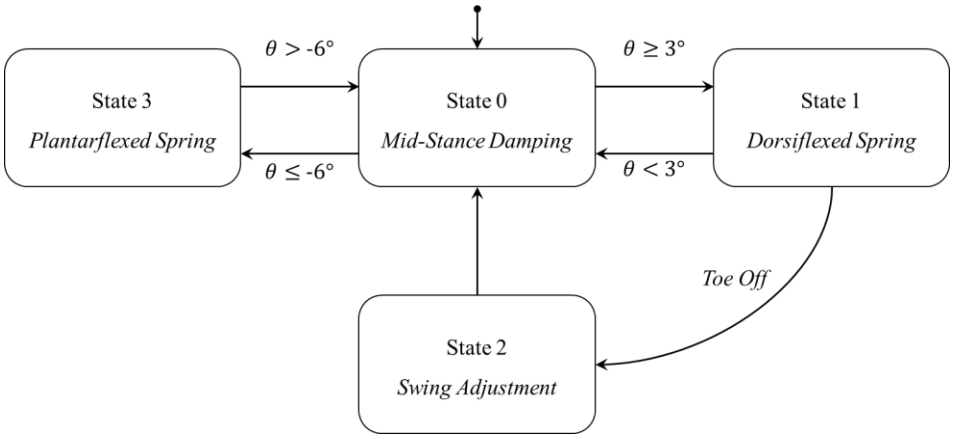

Figure 3. Finite State Machine for spring and damper controller

The third control scheme is an equilibrium-adjusting spring and damper controller. This controller emulates the behavior of the ankle developed and described in [1]. From heel strike through role-over, the torque is purely governed by damping to conform and provide smooth motion. From a determined equilibrium angle onward, the torque is transitioned into pure spring behavior, much like how Controller B engages a spring at a predefined angle. However, unlike Controller B, this angle is defined by the shank angle relative to the gravity vector rather than the relative ankle angle. Therefore, the spring equilibrium angle adjusts to an uphill or downhill slope to maintain the same angle relative to the body's position during rollover. This controller also utilizes a swing adjustment state to prevent toe scuffing. The FSM is shown below in Figure 4.

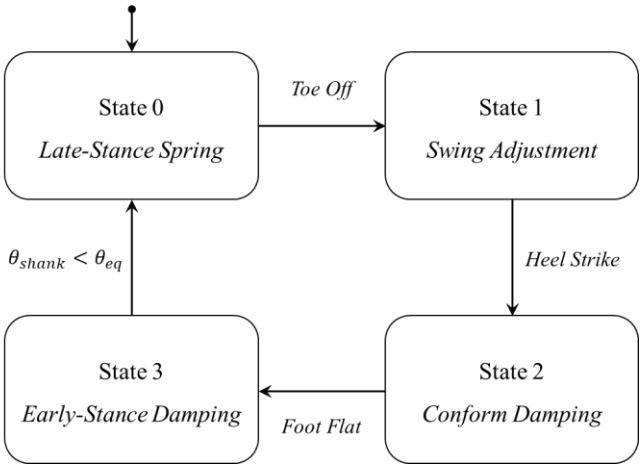

Figure 4. Finite State Machine for equilibrium-adjusting spring and damper controller

The robotic prosthesis has multiple control modes available to use, and for this study we implemented a real-time Simulink control. Controller A is set to constant values for k, b, and θ_{eq}, and Simulink is simply used to collect data feedback from the ankle control board. For Controllers B and C, a Stateflow chart is used to determine the proper values of k, b, and θ_{eq} at any point in the gait cycle and send these parameters to the ankle control board for torque calculation. In these controllers, Simulink is still used to collect data feedback, and all data communication between the Simulink controllers and the ankle prosthesis are performed over a CAN bus.

Methods

Study Participants

The three controllers were tested by three unilateral transtibial amputees, with ages ranging from 33 to 52 and weight ranging from 77.3 to 101.7 kilograms. All were of K level 3 or 4. Two participants were left side affected, and

one was right side affected. All three use passive prostheses for everyday living: both left side affected participants use the Fillauer AllPro, and the right side affected participant uses the Ottobock Challenger.

Experimental Protocol

For each participant, the study began with a tuning period. The stiffness was self-selected for Controller A while taking paces back and forth in a set of parallel bars. Once the subject felt comfortable with the settings, this same stiffness was transferred over to Controllers B and C. For Controller B, the damping during rollover/mid-stance was tuned to a comfortable setting, as well as the thresholds for detecting swing phase. For Controller C, both the damping coefficient during conformation/rollover and the angle at which the late-stance spring is engaged were tuned to the participant's preference.

Once the controller parameters were tuned, participants walked on a simple non-instrumented treadmill between the parallel bars. This allowed them to walk for a long enough time to develop a consistent rhythm, rather than only taking a few strides at a time. The participants walked on each controller for as long as needed until they felt comfortable with the behavior.

This process of tuning each controller and developing familiarity took one or two visits for each participant. On a subsequent visit, each participant was equipped with motion capture markers for kinematics

Figure 5. Participant walking with motion capture markers on instrumented treadmill at all three slopes

and kinetics data collection. Each participant conducted three 2-minute walking trials. Beginning with Controller A, the participant walked at 1.0 m/s on a 0° slope, followed by 0.8 m/s on a +6° slope, and then 0.8 m/s on a -6° slope. Images of a participant walking at each slope are shown in Figure 5. A higher speed was selected for level ground walking since people generally walk at higher speeds on level ground than on inclines when selecting their own pace. This set of level, up, and down slope walking was repeated with Controller B and then again with Controller C. For each trial, the first minute was used to achieve a comfortable steady state walk, and the second minute was used for data collection. The participants could take any breaks as needed during data collection.

Data Collection Equipment and Processing

The data collection allows for both kinematics and kinetics calculations. Joints and segments are tracked using a Vicon Nexus 10 camera motion capture system, with 40 markers covering each joint and segment from the waist down and 3 additional markers labeling the treadmill axes. The participants walk on a Bertec lateral split belt, force instrumented treadmill to measure ground reaction forces.

The Vicon Nexus software is used to label each marker in the experiment, after which we used C Motion's Visual3D software to perform inverse dynamics calculations to produce joint moments and angles, segment positions, and any other relevant metrics. The ground reaction force signal is zero phase filtered at a cutoff frequency of 15 Hz, and the markers' locations are zero phase filtered at a cutoff frequency of 10 Hz. The second minute of walking for each trial, which is used for this data analysis, is parsed into individual strides – heel strike to heel strike – normalizing each stride into one thousand points, and averaging them together to provide one normalized gait cycle for each trial.

The Visual3D torque and angular velocity curves were used to derive energy return. Ankle torque and angular velocity were multiplied to yield ankle power, which was then numerically integrated into ankle energy. This energy was divided by the participant's mass to normalize the data. From a plot of ankle energy, two metrics for energy return were easily derived. The total energy loss for each stride was found – which is the final value of ankle energy after toe off – as well as the push off energy – which is the difference between the total energy loss and minimum energy during stride.

To calculate a metric for symmetry of gait, we used the ratio of step length from toe off to heel strike (in meters) between the unaffected and affected side. To find this step length, the force plates were used to determine the time of each toe off and heel strike event. The motion capture data, which produces precise location of each segment in the treadmill frame, were used to find the location of each foot at the time of toe off and heel strike. This difference was added to the overall motion of either 1.0 m/s or 0.8 m/s multiplied by the time between toe off and heel strike. This calculation is summarized in (2), where v is the treadmill velocity, t_{HS} and x_{HS} are the time and foot position at heel strike, and t_{TO} and x_{TO} are the time and foot position at toe off.

$$Step\ Length = v \times (t_{HS} - t_{TO}) + (x_{HS} - x_{TO}) \tag{2}$$

This calculation was done for every step during the one minute trial, and then averaged for unaffected and affected side before finding the ratio.

For each subject, socket moment was calculated as the sagittal plane moment at the pyramid connector between the socket and prosthesis. The socket moment calculation, shown in (3), was found by linearly interpolating between the ankle torque and knee torque found from the Visual3D processing described above, with moments normalized by participant mass. The ankle and knee torques were only considered in the stance phase, since socket moment during swing is of less consequence to the users comfort. The shank was treated like a rigid body with a moment applied on each end, in which case the socket moment is proportional to the distance between the joints and the distance to the socket connector.

$$\tau_{socket} = \frac{\tau_{knee} - \tau_{ankle}}{l_{shank}} \times l_{socket} + \tau_{ankle} \tag{3}$$

τ_{socket}, τ_{knee}, and τ_{ankle} are the moment at the socket, knee, and ankle. l_{shank} and l_{socket} are the distance from the ankle joint to knee joint and the distance from the ankle joint to pyramid connector. This equation was used to generate both an average and a peak socket moment for each step.

Statistical Analysis

For each trial condition of slope and controller, the values for each parameter were calculated for each step, and all participants' steps were combined into a single data set. We ran a Kruskal-Wallis test to evaluate the statistical significance of differences in medians with controller type as the independent variable and the energy loss, energy return, symmetry of gait, and socket moment as dependent variables, grouping by slope.

Results

Energy Return

Figure 6 shows the results of prosthesis ankle energy throughout a normalized gait cycle for each controller on each slope. The curves plotted are representative strides, that is, a single stride that most closely represents the median values for net energy loss and push off energy. The calculated values of energy loss and push off energy for each condition are summarized in Table 1. The values listed are the medians from all strides by all participants, and after performing the Kruskal-Wallis tests, the statistical significance in difference is included. An asterisk indicates the median is significantly different from the other two controllers in that slope group.

Table 1. Summary of energy loss and return per step for each controller on each slope, normalized by participant mass. Statistical significance indicated with asterisks.

Slope	Controller	Energy Loss (J/kg $\times 10^{-1}$)	Push Off Energy (J/kg $\times 10^{-2}$)
-6° Decline	A	-1.291 *	4.82
	B	-1.709 *	4.48 *
	C	-1.288 *	4.78
0° Level	A	-1.478	6.39 *
	B	-2.078 *	2.29 *
	C	-1.638	4.60 *
+6° Incline	A	-1.112 *	8.82 *
	B	-1.201 *	7.20 *
	C	-1.017 *	5.74 *

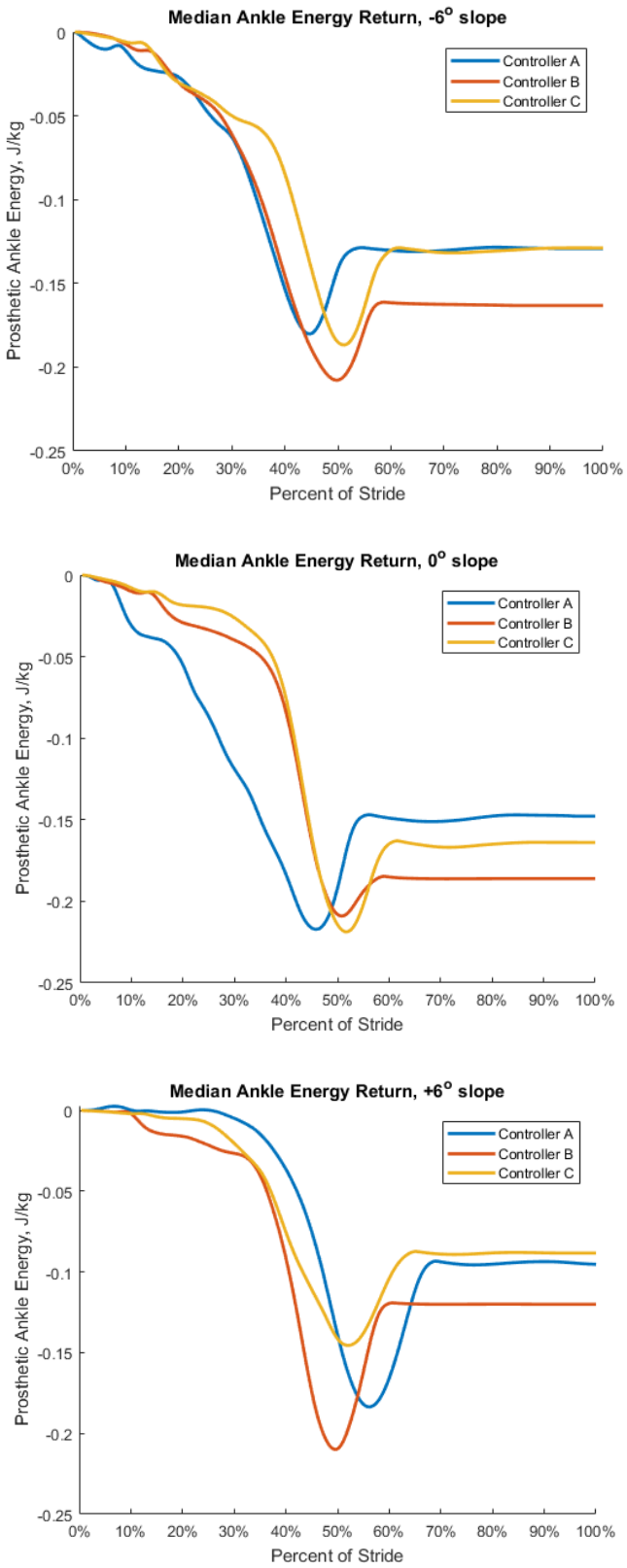

Figure 6. Comparing prosthetic ankle energy return for each controller, taking the median among all participants for (a) declined, (b) level, and (c) inclined slope

Symmetry of Gait

The symmetry of gait was calculated as described, taking the ratio of unaffected step length to affected step length. Steps were paired off to create a series of these ratios for each trial, and the total set of ratios for all participants is combined to perform the Kruskal-Wallis test within each slope condition. The results are shown in Figure 7, where the asterisk is used to indicate a case where the median symmetry of gait has a statistically significant difference from the other two controllers in that group.

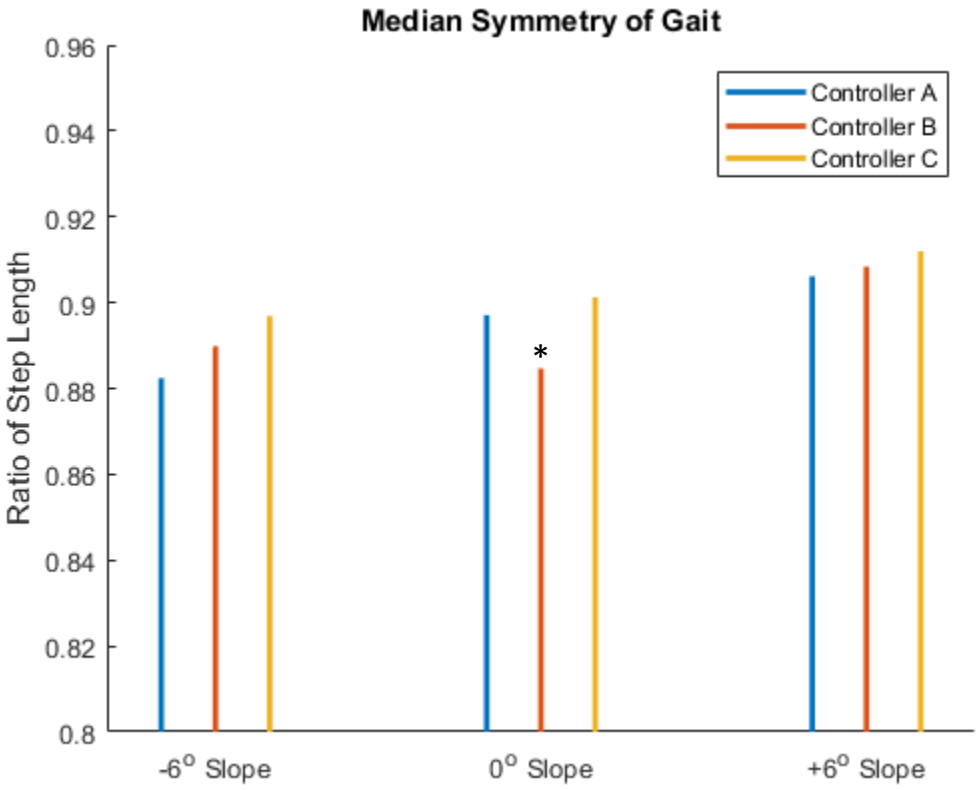

Figure 7. Symmetry of gait, taking the median of all participants together. Measured by a ratio between unaffected and affected step length, separated by slope and controller, with statistical significance marked.

Socket Moment

The socket moment was calculated as described for each stride of each trial. The average moment was taken for each stance for each trial, and the three participants stances are combined to take an overall median. Results for each condition are summarized in Figure 8. The peak moments for all strides of each condition are also combined

and the median is included for reference to reinforce trends. Again, the asterisks indicate a value that is found to have a statistically significant difference from both alternative controllers for that slope.

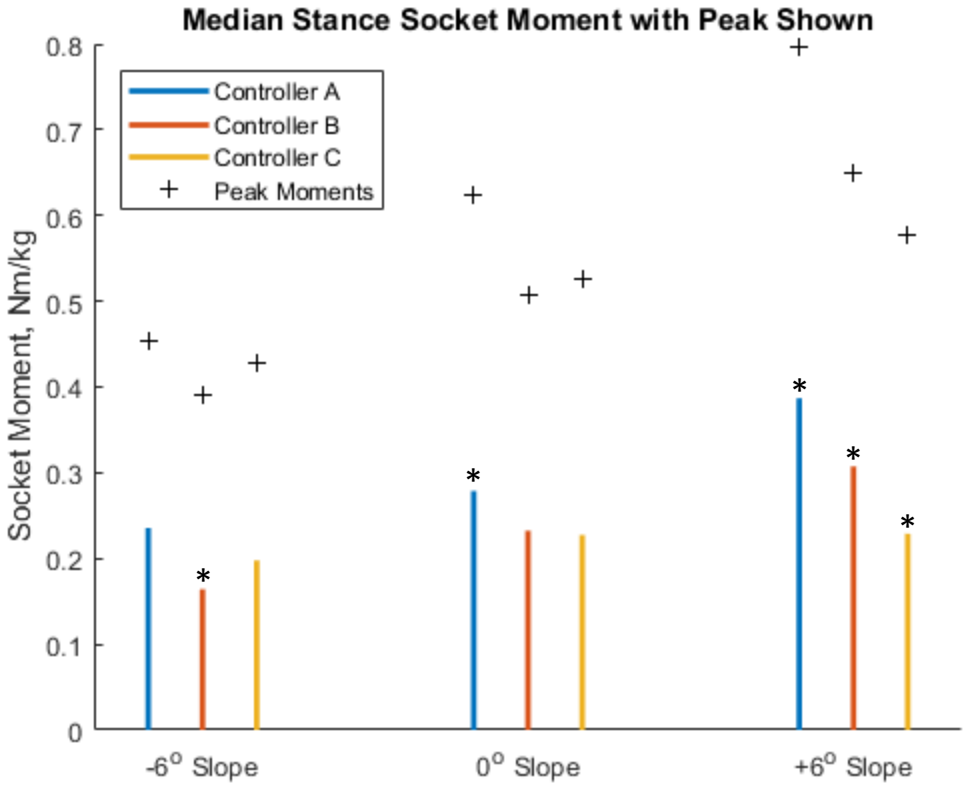

Figure 8. Average socket moment throughout stance for all participants averaged together, with average peak socket moment during stance included and statistical significance marked.

Discussion

Energy Return

From this data, the energy return hypotheses have been largely validated. In all cases, Controller B demonstrated greater energy loss and lower push off energy than Controller A. The overall energy loss is in part due to the greater energy dissipated by the damping in mid-stance, and the reduced push off energy can be explained in part by the more dorsiflexed equilibrium angle of the spring. Controller C demonstrates the least energy loss in all cases except for on level ground, where it was not significantly different from Controller A. It also demonstrates improved push off energy from Controller B in the decline and level conditions, likely due to the spring stage engaging at an earlier angle in stance. While it does not provide larger push off energy in the incline condition, this

is likely because the equilibrium angle is adapting to the slope. The steeper slope leads to a more dorsiflexed equilibrium angle, therefore reducing the amount of spring compression before push off, and it still provides improved net energy loss. These findings are mostly consistent with [10], showing that a multifunctional prosthesis can provide more negative work on ramp decent, and with [2], finding that multifunctional prostheses often reduce the overall energy return in favor of other benefits. Controller C, however, can provide comparable energy return benefits as Controller A while still utilizing a damping phase for smoother conformation and roll-over.

Symmetry of Gait

While there are some trends present that align with the hypotheses for symmetry of gait, in most cases there is a lack of statistical significance and a need for more data. The instance that is shown to be significant is that Controller B has a significantly lower ratio of step lengths compared to Controller A and C on level ground. This trend was also shown on declines for two of the participants, but none of the participants had significant differences for inclined walking. Since Controller B has a later engagement angle, effectively shortening the roll-over radius, it makes sense to see a trend of less symmetry between steps for Controller B. This effect would have the most effect on level ground, where an equilibrium angle near zero degrees is more advantageous, while a more dorsiflexed angle is beneficial on inclines. As the statistical analysis shows, there is not a conclusive difference for sloped walking, and there is some variance by participant. From other studies that evaluate other metrics for symmetry of gait [2] [4] [5], there are more factors influencing this than rollover shape, and in fact the hydraulic damping can improve some measures of symmetry.

Socket Moment

The hypothesis was confirmed for many conditions: adding a damping phase to the gait cycle can significantly reduce socket moment during stance. Controller B demonstrated significantly lower socket moments than Controller A at all slopes, and Controller C was also significantly reduced for level ground and inclined walking. Controller C produced even lower socket torques during inclined walking than Controller B, which demonstrates the benefit of adjusting the spring engagement angle to match the slope. On slopes steeper than the 3^{o} dorsiflexed angle that Controller B engages its spring at, being able to shift the equilibrium angle even further allows for reduced socket torque while still providing a decent energy return.

Limitations

The primary limitations of this study come from the sample size of participants and prosthesis emulator. As the experiment was only conducted with 3 participants, even though there are statistically significant results, they must be considered in the context of a limited sample. The gait behaviors of individuals can largely affect the human-prosthesis interaction to produce differing results. The use of the prosthesis emulator also yields some limitations. For one, using the same prosthesis for all behaviors controls for weight, helping to isolate the behaviors themselves for tradeoff. However, this eliminates one of the larges advantages of carbon fiber spring feet, which is their light weight. The weight of transtibial prostheses, being as distal on the limb as they are, has a large impact on biomechanics. Despite the added mass, we do not expect mass to influence the outcome measures for this study. Additionally, the high transmission ratio of the prosthesis produces a large rotor inertia, which causes some added torques when changing directions – especially from foot conformation to roll-over. The friction in this transmission also causes some energy losses that a standard carbon fiber foot would lack.

Conclusion

Many groups are developing multifunctional prostheses to provide added benefits as compared to a simple spring foot. This study has found that some such control schemes can indeed reduce the socket moment during stance and absorb more energy during downhill walking, but also may reduce push off energy and, in some cases, symmetry of step length. By having an adjustable equilibrium angle to transition from a damping phase to a push off spring, such controllers may be able to maintain energy delivery similar to a spring foot but with the benefit of reduced loads for the user. While multifunctional prostheses can provide biomechanical advantages, one of the greatest disadvantages of such prostheses remains weight. This study controlled for weight in order to isolate the controller behaviors themselves, but actual simple spring prostheses remain lighter than many multifunctional prostheses. As multifunctional prostheses become more efficient in design and lighter in weight, they can become a more consistently preferred option, especially for tasks other than simple level ground walking.

References

[1] H. L. Bartlett, B. E. Lawson and M. Goldfarb, "Design, Control, and Preliminary Assessment of a Multifunctional Semi-Powered Ankle Prosthesis," *IEEE/ASME Transactions on Mechatronics,* doi: 10.1109/TMECH.2019.2918685.

[2] A. R. De Asha, R. Munjal, J. Kulkarni and J. G. Buckley, "Impact on the biomechanics of overground gait of using an'Echelon'hydraulic ankle–foot device in unilateral trans-tibial andtrans-femoral amputees," *Clinical Biomechanics,* vol. 29, no. 7, pp. 728-734, Aug. 2014.

[3] A. R. De Asha, L. Johnson, R. Munjal, J. Kulkarni and J. G. Buckley, "Attenuation of centre-of-pressure trajectory fluctuations under the prosthetic foot when using an articulating hydraulic ankle attachment compared to fixed attachment," *Clinical Biomechanics,* vol. 28, no. 2, pp. 218-224, Feb. 2013,.

[4] A. R. De Asha, R. Munjal, J. Kulkarni and J. G. Buckley, "Walking speed related joint kinetic alterations in trans-tibial amputees: impact of hydraulic 'ankle' damping," *Journal of NeuroEngineering and Rehabilitation,* vol. 10, no. 107, pp. 1-15, Oct. 2013.

[5] R. Moore, "Effect on Stance Phase Timing Asymmetry in Individuals with Amputation Using Hydraulic Ankle Units," *Journal of Prosthetics and Orthotics,* vol. 28, no. 1, pp. 44-48, Jan. 2016.

[6] L. Johnson, A. R. De Asha, R. Munjal, J. Kulkarni and J. G. Buckley, "Toe clearance when walking in people with unilateral transtibial amputation: Effects of passive hydraulic ankle," *Journal of Rehabilitation Research and Development,* vol. 51, no. 3, pp. 429-438, 2014.

[7] N. Alexander, G. Strutzenberger, J. Kröll, J. Christian, T. Wunsch and H. Schwameder, "Joint loading during graded walking with different prostheses - a case study," in *1st Clinical Movement Analysis World Conference*, Rome, 2014.

[8] L. Fradet, M. Alimusaj, F. Braatz and S. I. Wolf, "Biomechanical analysis of ramp ambulation of transtibial amputees with an adaptive ankle foot system," *Gait & Posture,* vol. 32, no. 2, pp. 191-198, June 2010.

[9] S. R. Koehler-McNicholas, E. A. Nickel, J. Medvec, K. Barrons, S. Mion and A. H. Hansen, "The influence of a hydraulic prosthetic ankle on residual limb loading during sloped walking," *PLOS ONE,* vol. 12, no. 3, pp. 1-18, March 2017.

[10] V. Struchkov and J. G. Buckley, "Biomechanics of ramp descent in unilateral trans-tibial amputees: Comparison of a microprocessor controlled foot with conventionalankle–foot mechanisms," *Clinical Biomechanics,* vol. 32, pp. 164-170, Feb. 2016.

[11] S. Portnoy, A. Kristal, A. Gefen and I. Siev-Ner, "Outdoor dynamic subject-specific evaluation of internal stresses in the residual limb: Hydraulic energy-stored prosthetic foot compared to conventional energy-stored prosthetic feet," *Gait & Posture,* vol. 35, no. 1, pp. 121-125, Jan. 2012.

[12] R. Moore, "Effect of a Prosthetic Foot with a Hydraulic Ankle Unit on the Contralateral Foot Peak Plantar Pressures in Individuals with Unilateral Amputation," *Journal of Prosthetics and Orthotics,* vol. 30, no. 3, pp. 165-170, July 2018.

[13] A. H. Shultz, B. E. Lawson and M. Goldfarb, "Variable Cadence Walking and Ground Adaptive Standing With a Powered Ankle Prosthesis," *IEEE Transactions on Neural Systems and Rehabilitation Engineering,* vol. 24, no. 4, pp. 495-505, April 2016.